Dynamics, Rectification, and Fractionation for Colloids on Flashing Substrates

A. Libál,[1,2] C. Reichhardt,[1] B. Jankó,[2] and C. J. Olson Reichhardt[1]

[1]*Center for Nonlinear Studies and Theoretical Division, Los Alamos National Laboratory, Los Alamos, New Mexico 87545, USA*

[2]*Department of Physics, University of Notre Dame, Notre Dame, Indiana 46556, USA*

(Received 11 August 2005; published 10 May 2006)

We show that a rich variety of dynamic phases can be realized for mono- and bidisperse mixtures of interacting colloids under the influence of a symmetric flashing periodic substrate. With the addition of dc or ac drives, phase locking, jamming, and new types of ratchet effects occur. In some regimes we find that the addition of a nonratcheting species *increases* the velocity of the ratcheting particles. We show that these effects occur due to the collective interactions of the colloids.

DOI: 10.1103/PhysRevLett.96.188301 PACS numbers: 82.70.Dd

The motion and ordering of colloidal particles on two-dimensional (2D) periodic substrates has been attracting growing interest due to recent experimental breakthroughs that permit the creation of static 1D and 2D periodic substrate arrays using optical and holographic techniques [1–8]. It is also possible to create *dynamic* periodic arrays, such as flashing or shifting traps [1,9–11]. Colloidal particles interacting with periodic substrates are ideal model systems for studying general problems in condensed matter physics, such as the ordering and melting of commensurate and incommensurate elastic lattices on periodic surfaces. Problems of this type can arise in vortex crystal ordering in superconductors [12] or Bose-Einstein condensates (BECs) with periodic pinning sites [13] as well as molecules adsorbed on surfaces [14]. The dynamics of colloids moving over periodic substrates is also relevant to understanding depinning phenomena [6,15] and phase locking [4]. In addition to the scientific interest in these systems, there are technical applications for colloids moving over periodic arrays, such as the fractionation or segregation of colloidal mixtures [4,5,7–9]. For example, species fractionation can be achieved by flowing colloidal mixtures over an array at an angle such that the motion of one colloid species locks to a symmetry direction of the periodic array while the other species moves in the driving direction [4,7,8]. Other segregation phenomena occur when the substrate is dynamic, and rectification or ratchet devices can be constructed in which one species ratchets at a different velocity than the other [10]. New ratchet-based logic devices have also been realized [11] which may be useful for understanding similar solid state nanoscale devices [16].

Assemblies of interacting particles have been extensively studied for systems with random disorder and periodic substrates. Collectively interacting particles on a flashing substrate is a new class of problem that can be realized experimentally using dynamic substrates. For particles interacting with optical traps, flashing can be achieved simply by modulating the laser power. It should be possible to create similar flashing potentials for vortices in BECs or ions interacting with optical arrays [13].

In this work we consider mono- and bidisperse assemblies of charged colloids interacting with flashing 2D symmetric periodic substrates. When a dc drive is applied to this system, phase locking in the velocity-force curves occurs. If an external ac drive is applied instead of a dc drive, we find that new types of ratchet effects can be realized. For bidisperse colloidal assemblies, the relative velocity between the two colloid species is affected by the density, number ratio, and charge disparity of the species. We find that collective effects play an important role in the ratcheting behavior. For a system containing a nonratcheting species A, the introduction of a second species B that does ratchet can induce ratcheting in species A due to the interactions between the colloid species. The effectiveness of the induced ratcheting goes through a peak as the fraction of ratcheting particles is changed at fixed colloid density. At high densities, the colloids reach a *jammed* state and both species ratchet at the same velocity. We also find a remarkable phenomenon for strongly interacting particles, where it is possible to *increase* the drift velocity of a ratcheting species by adding nonratcheting colloids to the system. This effect occurs when the disorder introduced by the nonratcheting species breaks apart structures formed by the ratcheting species and allows the latter to couple more effectively to the substrate. Our results can be tested experimentally for colloids interacting with flashing optical traps.

We consider a 2D Brownian dynamics (BD) simulation of N interacting colloids with periodic boundary conditions in both the x and y directions. We neglect hydrodynamic and excluded volume interactions, which are reasonable assumptions for strongly charge-stabilized particles in the low volume fraction limit. The overdamped equation of motion [17] for colloid i is given by

$$\eta \frac{d\mathbf{R}_i}{dt} = \mathbf{F}_i^{\mathrm{cc}} + \mathbf{F}_i^{T} + \mathbf{F}_i^{s} + \mathbf{F}_i^{\mathrm{ext}}, \tag{1}$$

where the damping constant η is set to unity. The colloid-colloid interaction force is $\mathbf{F}_i^{\mathrm{cc}} = q_i \sum_{i \neq j}^{N_i} -\nabla_i V(r_{ij})$, where the colloid-colloid potential is a Yukawa or screened Coulomb interaction with the form $V(r_{ij}) = E_0(q_j/|\mathbf{r}_i - \mathbf{r}_j|)\exp(-\kappa|\mathbf{r}_i - \mathbf{r}_j|)$. Here, $E_0 = Z^{*2}/(4\pi\epsilon\epsilon_0)$, where

charge is measured in units of Z^* and ϵ is the solvent dielectric constant. Lengths are measured in units of a_0, assumed of order a micron, while time and force are measured in units of $\tau = \eta/E_0$ and $F_0 = E_0/a_0$. $q_{j(i)}$ is the charge on particle $j(i)$, $1/\kappa$ is the screening length which is set to $2a_0$, and $\mathbf{r}_{i(j)}$ is the position of particle $i(j)$. For monodisperse assemblies, $q_i/q_j = 1$, while for bidisperse assemblies, $q_i/q_j \neq 1$. The thermal force $\mathbf{F}^T$ is modeled as random Langevin kicks with the properties $\langle \mathbf{F}_i^T \rangle = 0$ and $\langle \mathbf{F}^T(t)\mathbf{F}^T(t') \rangle = 2\eta k_B T \delta(t - t')$. The substrate force $\mathbf{F}_i^s = A \sin(2\pi x/a_x)\hat{\mathbf{x}} + B \sin(2\pi y/a_y)\hat{\mathbf{y}}$ with N_p minima is flashed on and off with a square wave that has a 50% duty cycle beginning in the off state at $t = 0$. Here $a_x = 4a_0$ is the substrate periodicity, $a_y = \sqrt{3}a_x/2$, $A = B$ is the strength of the substrate, T_s is the flashing period, and $\omega_s = 2\pi/T_s$. For most of this work, the sample size is $76a_0 \times 65.8a_0$. The term $\mathbf{F}_i^{\rm ext}$ represents an externally applied drive. For a dc drive, $\mathbf{F}_i^{\rm ext} = F^{\rm dc}\hat{\mathbf{x}}$, and for an ac drive of frequency ω_d, phase offset ϕ, and no force off set from zero, $\mathbf{F}_i^{\rm ext} = F^{\rm ac} \sin[(\omega_d + \phi)t]\hat{\mathbf{x}}$. We allow the system to reach a steady state, which takes less than 5000 BD steps, before measuring the time-averaged particle velocities of each species, $\langle V_{A(B)} \rangle = (\tau_{\rm av} N_{A(B)})^{-1} \times \sum_{i=1}^{N_{A(B)}} \sum_{t=0}^{\tau_{\rm av}} \hat{\mathbf{x}} \cdot \mathbf{v}_i(t)$, where $\tau_{\rm av} > T_s$, $\tau_{\rm av} = 5000$ to 1×10^6 BD steps.

We first consider the case of monodisperse colloidal assemblies interacting with a flashing substrate and a dc drive, where we find phase locking. For a particle moving over a periodic substrate with an additional ac drive, phase locking takes the form of Shapiro steps [18], in which the particle velocity is periodically modulated by the dc motion over the substrate at a frequency $\omega_m = a_x\eta/(F^{\rm dc}\tau)$. When $\omega_m = n\omega_d$, with n an integer, a synchronization of frequencies occurs and the particle motion stays locked at the same dc velocity over a range of dc drive, producing steps in the velocity-force curve. In our system we consider a dc drive and a flashing substrate, and there is no external ac driving force. The synchronization occurs as $\omega_m = n\omega_s$. Here, the flashing substrate permits the realization of phase locking without an external ac drive.

In Fig. 1(a) we show a series of velocity-force curves for varied ω_s for the case $N = N_p$. A depinning threshold appears at $F^{\rm dc} = 0.34$ followed by a series of phase locking steps. For higher ω_s, steps at higher $F^{\rm dc}$ can be resolved. In Fig. 1(b) we plot the velocity-force curves for varied substrate strength A at fixed $T_s = 300$. Larger numbers of steps that have a saturated width appear for larger A. These saturated steps are distinct from Shapiro steps, where the width of the nth step varies with ac amplitude as the nth-order Bessel function. For $F^{\rm dc} > A$, particles are no longer trapped in the minima when the substrate cycles on, and much weaker Shapiro steps appear. When the number of colloids is incommensurate with the substrate, the steps become smooth and have a finite slope as additional soliton type pulses of motion are present which do not lock to ω_s.

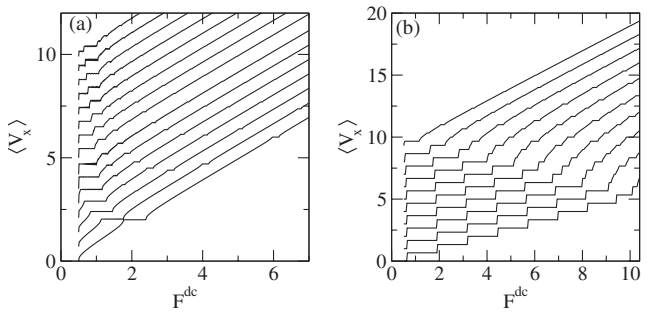

FIG. 1. (a) $\langle V_x \rangle$ vs $F^{\rm dc}$ for a system with $N/N_p = 1$ and $N_p = 361$ for $A = 1$ at varied flashing period. From bottom to top, $T_s = 100$, 150, 200, 250, 300, 350, 400, 450, 500, 550, 600, 650, 700, 750, and 800 BD steps. (b) Same as in (a), with a fixed $T_s = 300$ and increasing substrate strength A. From top to bottom, $A = 1$, 2, 3, 4, 5, 6, 7, 8, 9, and 10. All curves have been vertically offset for clarity.

If an ac drive is applied instead of a dc drive, it is possible to produce a ratchet effect. Consider the case where $F^{\rm ac} < A$, such that if the substrate potential were static, the particle would remain trapped within a single pinning plaquette. The particle is able to move under the influence of the ac drive during the period of time when the substrate flashes off, but will be trapped in whichever plaquette it reached when the substrate flashes back to the on state. Depending on the amplitude, frequency ω_d, and phase of the ac drive relative to the flashing of the substrate, the particle may be able to move forward a distance na in the x direction with each cycle of the pinning, where n is an integer, but is trapped inside a pin during part or all the period of time when it would otherwise have moved a distance $-na$, resulting in a net dc motion. In Fig. 2(a) we show the average velocity in the x direction $\langle V_x \rangle$ vs $F^{\rm ac}$ for a system with $\omega_s/\omega_d = 1$, $N_p = 64$, and $\phi = 0$. For the commensurate case of $N = 64$, the effective ratchet velocity goes through a series of peaks of decreasing height, with the maximum peak occurring at $F^{\rm ac} = 1.25$. Between the peaks, $\langle V_x \rangle \approx 0$. The decreasing envelope of peak heights with increasing $F^{\rm ac}$ arises since the particles are able to depin during part of the cycle when the pins have flashed to the on state, decreasing the net rectification. At incommensurate fillings $N \neq N_p$, the colloid positions are more disordered due to the colloid-colloid interaction forces and the rectification peaks become smeared. In Fig. 2(b) we plot results from a larger system of 19×19 pins at the same a_x. At $N/N_p = 1$, peaks again appear as a function of $F^{\rm ac}$, while at the higher colloid densities the peaks are smoothed. The peak height is constant for $N/N_p \leq 1$, since at submatching densities, particle-particle interactions do not play an important role and the rectification that occurs is a strictly single-particle process. In the inset of Fig. 2(b) we show the monotonic decrease for the maximum peak value of $\langle V_x \rangle$ for increasing N/N_p, which can be fitted well to an exponential decay. The ratchet effect also depends on the phase ϕ

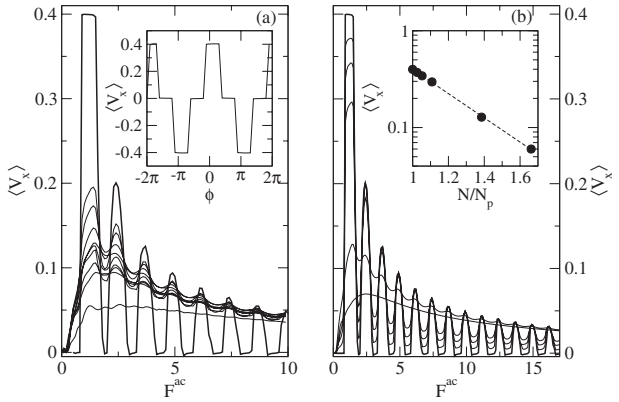

FIG. 2. (a) $\langle V_x \rangle$ vs F^{ac} for a system with $\omega_s/\omega_d = 1$ and $N_p = 64$. From top to bottom maximum, $N/N_p = 1$, 1.25, 1.28, 1.33, 1.375, 1.41, 1.44, 1.47, 1.5, and 2.0. Inset: $\langle V_x \rangle$ for the same system in (a) for varied phase difference ϕ between the ac drive and flashing substrate. (b) Same as in (a) for a higher $N_p = 361$ with $N/N_p = 1$ (top peak), 1.025, 1.05, 1.10, 1.39, and 1.66 (bottom smooth curve). Inset: the maximum value of $\langle V_x \rangle$ vs N/N_p for the system in (b).

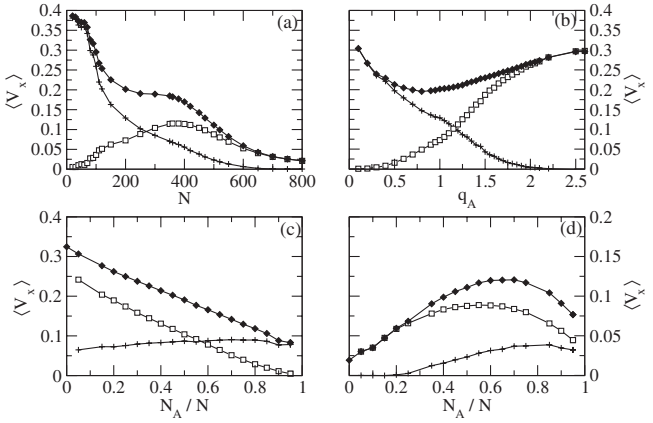

FIG. 3. Ratcheting effect for colloidal mixtures in a sample with $N_p = 722$. Open squares: $\langle V_x^A \rangle$ for nonratcheting species A; solid diamonds: $\langle V_x^B \rangle$ for ratcheting species B; plus symbols: relative velocity. (a) Fixed $N_A/N = 1/2$ for increasing N. (b) Fixed $N_A/N = 1/2$, $N = 200$, and $q_B = 3$ for increasing q_A. (c) Fixed $N = 300$ and increasing N_A/N. (d) Fixed $N = 500$ and increasing N_A/N.

between the flashing pinning and ac driving force. In the inset of Fig. 2(a) we show V_x vs ϕ for a fixed $F^{ac} = 1.0$. V_x is positive for $\phi = 0$, zero near $\phi = \pi/2$, and negative for $\phi = \pi$.

We next consider mixtures of two colloidal species with different charge. The coupling to the ac drive is weaker for the species with smaller charge. We first show how the density of the system affects the ratcheting for an ac drive at which species B with charge $q_B = 3$ ratchets and species A with charge $q_A = 1$ does not. In Fig. 3(a) we plot the average velocities $\langle V_x^A \rangle$ and $\langle V_x^B \rangle$ vs N, with fixed $N_A/N = 1/2$, $A = 1.0$, $T_s = T_d = 500$, and $q_B/q_A = 3$. For low densities, species B moves at a finite velocity while $\langle V_x^A \rangle$ is close to zero. As N increases, the particles interact more strongly and the ratcheting particles B push the A particles forward, inducing a ratcheting effect for species A. In Fig. 4(a) we illustrate the motion of the colloidal mixtures at a low density. All of the species B particles are mobile, as indicated by the trajectories. In several places species A particles can be seen to be immobile. However, in the middle and right portions of the figure, two A particles have trails indicating motion that was produced as a species B particle pushed the species A particle. This is the mechanism which causes the ratcheting in species A. We note that if only species A is present, no ratchet effect occurs for any value of N unless F^{ac} is increased. The removal of the last few B particles slows the system in a nonlinear fashion until the whole system stops at $N_A/N = 1$.

As the total number of particles increases for fixed $N_A/N = 1/2$, shown in Fig. 3(a), $\langle V_x^B \rangle$ drops as more of the ratcheting energy is transferred to species A. We find a maximum in $\langle V_x^A \rangle$ at $N \approx 400$. The velocity of both species decreases for $N > 400$. For $N > 700$ the system jams and the particles can no longer exchange positions, so both species move with the same velocity. In Fig. 4(b) at $N = 700$, the species tend to clump together, with species B tending to form crystallites. The jamming or freezing transition we find is similar to the freezing at increased density observed in systems of two species of particles moving in different directions [19].

In Fig. 3(a), the relative velocity $\langle V_x^B \rangle - \langle V_x^A \rangle$ between species A and B is a measure of the fractionation, and it

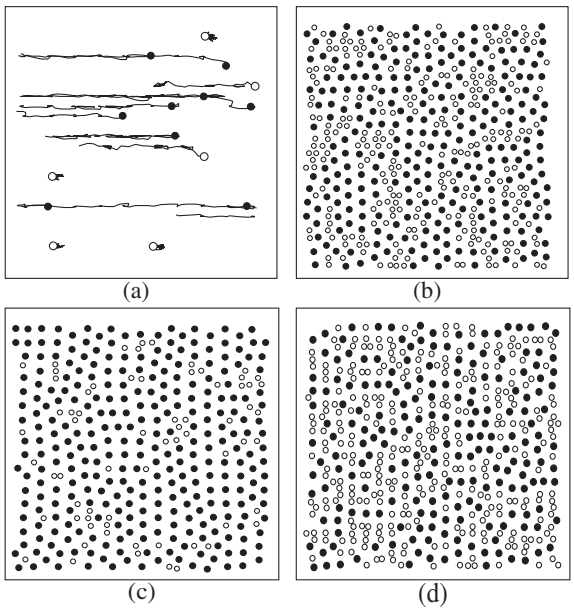

FIG. 4. Snapshot of colloid positions (circles) and trajectories (lines) in a portion of the sample for a fixed period of time for the system in Fig. 3(a) at $N = 40$. Dark circles are the ratcheting species B and light circles are the nonratcheting species A. (b) Snapshot of the jammed system in Fig. 3(a) at $N = 700$. (c) Snapshot at $N_A/N = 0.2$ in Fig. 3(d). (d) Snapshot at $N_A/N = 0.6$ in Fig. 3(d).

drops to zero when the system jams. In Fig. 3(b) we plot $\langle V_x^A \rangle$ and $\langle V_x^B \rangle$ vs varied charge q_A for the same system in Fig. 3(a) at fixed density with $N = 200$. Here $\langle V_x^A \rangle$ increases monotonically with q_A, and for $q_A > 2.5$, the velocities of the two species are the same. $\langle V_x^B \rangle$ decreases with increasing q_A for $q_A < 1.0$ since species A needs to be pushed in order to ratchet for these values of q_A, and the coupling between the species increases with q_A, resulting in a larger drag on species B. For $q_A > 1$, the A species starts to ratchet on its own and $\langle V_x^B \rangle$ recovers as the drag from species A diminishes.

In Fig. 3(c) for a low density at $N = 300$ we show V_x as a function of N_A/N. As the fraction of ratcheting colloids goes to zero, the velocity of both species is monotonically reduced. In the low density regime the system is always liquidlike. In Fig. 3(d) we show a very different behavior at a much higher $N = 500$. Here, increasing the fraction of nonratcheting particles N_A/N *increases* the average velocity of *both* the ratcheting and nonratcheting species. The relative velocity between the two species also increases for higher N_A/N. These effects are more pronounced for higher N. For small N_A/N at high densities, the colloid-colloid interactions dominate and the system acts as a rigid unit so that all the colloids must ratchet at the same velocity together, as in Fig. 4(c). In general some colloids fall at locations that are incommensurate with the substrate, so they do not ratchet as effectively and slow the entire system. In Fig. 3(d) for low N_A/N, $\langle V_x^A \rangle = \langle V_x^B \rangle$, indicating that the system is moving elastically. For higher fractions the velocities differ, indicating that tearing of the lattice occurs, and at the same time the velocities of both species increase. We observe that in this case the system is much more disordered and the colloids act more as single particles rather than as a collective unit. Thus, the addition of the nonratcheting particles effectively breaks up the system or adds disorder, as in Fig. 4(d), which allows the system to behave as a liquid rather than a solid. This improves the coupling of the ratcheting colloids to the substrate since they are no longer held in incommensurate positions, and increases the overall effectiveness of the ratcheting. We have also performed extensive simulations for other parameters such as varied ratios of A and B, changing the steepness of the substrate potentials, densities, N_A/N, and T. In all cases we find the same general features of the ratchet effects described here, leading us to believe that the effects are very generic.

To summarize, we have shown that a variety of dynamical behaviors, including phase locking, ratchet effects, and jamming, are possible for colloids and colloidal mixtures interacting with flashing symmetric periodic substrates. For a flashing substrate with a dc drive, a phase locking occurs that is distinct from the typically studied Shapiro step phase locking. If a strictly ac drive is applied to a flashing substrate, a ratchet effect can occur, with a ratcheting direction that depends on the relative phase of the two ac signals. For mixtures of particles in regimes where one species ratchets and the other does not, we show that the ratcheting species can induce a ratchet effect in the nonratcheting species, at the cost of a reduced effectiveness of ratcheting in the first species. For high densities the system jams and both species move at the same velocity. We have demonstrated the ratchet effect for a wide range of parameters for the mixtures. In the dense regime we find that adding nonratcheting colloids can *increase* the drift velocity of the ratcheting species. This is due to the nonratcheting particles breaking up the elastic flow of the ratcheting species and improving the coupling to the substrate. Our results should be readily testable for colloids on dynamical optical traps.

This work was supported by the US Department of Energy under Contract No. W-7405-ENG-36. B. J. was supported by the NSF-NIRT Grant No. DMR-02-10519 and by the Alfred P. Sloan Foundation.

[1] D. G. Grier, Nature (London) **424**, 810 (2003).
[2] M. Brunner and C. Bechinger, Phys. Rev. Lett. **88**, 248302 (2002); K. Mangold, P. Leiderer, and C. Bechinger, *ibid.* **90**, 158302 (2003).
[3] C. Reichhardt and C. J. Olson, Phys. Rev. Lett. **88**, 248301 (2002).
[4] P. T. Korda, M. B. Taylor, and D. G. Grier, Phys. Rev. Lett. **89**, 128301 (2002).
[5] K. Ladavac, K. Kasza, and D. G. Grier, Phys. Rev. E **70**, 010901(R) (2004); M. Pelton, K. Ladavac, and D. G. Grier, *ibid.* **70**, 031108 (2004).
[6] P. T. Korda, G. C. Spalding, and D. G. Grier, Phys. Rev. B **66**, 024504 (2002).
[7] M. P. MacDonald, G. C. Spalding, and K. Dholakia, Nature (London) **426**, 421 (2003).
[8] J. Gluckstad, Nat. Mater. **3**, 9 (2004).
[9] B. A. Koss and D. G. Grier, Appl. Phys. Lett. **82**, 3985 (2003).
[10] S. H. Lee, K. Ladavac, M. Polin, and D. G. Grier, Phys. Rev. Lett. **94**, 110601 (2005); S. H. Lee and D. G. Grier, Phys. Rev. E **71**, 060102(R) (2005).
[11] D. Babic and C. Bechinger, Phys. Rev. Lett. **94**, 148303 (2005); D. Babic, C. Schmitt, and C. Bechinger, Chaos **15**, 026114 (2005).
[12] K. Harada *et al.*, Science **274**, 1167 (1996).
[13] J. W. Reijnders and R. A. Duine, Phys. Rev. Lett. **93**, 060401 (2004); H. Pu, L. O. Baksmaty, S. Yi, and N. P. Bigelow, *ibid.* **94**, 190401 (2005).
[14] A. B. Harris and A. J. Berlinsky, Can. J. Phys. **57**, 1852 (1979).
[15] C. Reichhardt and C. J. Olson Reichhardt, Europhys. Lett. **68**, 303 (2004).
[16] M. B. Hastings, C. J. Olson Reichhardt, and C. Reichhardt, Phys. Rev. Lett. **90**, 247004 (2003).
[17] D. L. Ermack and J. A. McCammon, J. Chem. Phys. **69**, 1352 (1978).
[18] S. Shapiro, Phys. Rev. Lett. **11**, 80 (1963); for a review, see: R. L. Kautz, Rep. Prog. Phys. **59**, 935 (1996).
[19] D. Helbing, I. J. Farkas, and T. Vicsek, Phys. Rev. Lett. **84**, 1240 (2000).